



SDMBCv2 (v1.0): correcting systematic biases in RCM inputs for future projection

Youngil Kim¹, Jason P. Evans^{1,2}

¹ Climate Change Research Centre, University of New South Wales, Sydney, New South Wales, Australia

² ARC Centre of Excellence for the Weather of the 21st Century, University of New South Wales, Sydney, New South Wales, Australia

Correspondence to: Youngil Kim (youngil.kim@unsw.edu.au)

Abstract. Regional Climate Models (RCMs) offer enhanced spatial resolution and a more realistic depiction of local climate processes. However, they often inherit systematic biases from their driving Global Climate Models (GCMs), which can compromise the accuracy of downscaled climate projections. To address this, bias correction techniques have been widely employed to adjust GCM and RCM outputs, particularly for climate impact and adaptation studies. Traditional methods, however, typically correct surface variables independently and lack physical and dynamical consistency. Bias correcting GCM boundary conditions prior to RCM simulation ensures a more coherent, physically and dynamically consistent, regional climate simulation with reduced errors. This study evaluates the effectiveness of such an approach using a calibration/validation framework, demonstrating significant error reduction during the validation (out-of-sample) period compared to uncorrected GCM data. We present an updated version of the open-source Python package, *Sub-Daily Multivariate Bias Correction (SDMBC) v2*, designed to correct RCM input variables using both reanalysis and raw GCM datasets. Enhancements include support for future climate projections, flexible horizontal and vertical interpolation for compatibility with diverse datasets, and a fully Python-based architecture optimized for parallel processing and high-performance computing. This paper illustrates the software's capabilities and provides a practical application example.

1. Introduction

The growing need to address the limitations of Global Climate Models (GCMs) in regional and hydrological contexts has led to the widespread use of downscaling approaches. These methods refine coarse-resolution GCM outputs into finer resolutions suitable for regional applications, such as water resource management and climate change adaptation. Dynamical downscaling employs Regional Climate Models (RCMs) with boundary conditions derived from GCMs, offering a more realistic representation of local physical processes that influence variables such as near-surface air temperature and precipitation. The enhanced resolution provided by RCMs aids in designing new infrastructure standards, assessing water vulnerability, evaluating drought risk, and gaining crucial insights into human health risks.



Despite the advantages of RCMs, they inherit biases from the driving GCMs, resulting in significant errors and artifacts that can diminish the benefits of dynamical downscaling (Rocheta et al. (2017); Kim et al. (2021); Risser et al. (2024)). The propagation of GCM biases into RCM outputs through the RCM input boundaries raises concerns about the fidelity and reliability of future climate projections. To address this issue, bias correction techniques have been developed and widely applied.

In the context of dynamical downscaling, bias correction can be implemented either before or after running the RCM. Post-downscaling bias correction can be applied to the variables of interest to climate data users, such as surface air temperature and precipitation. This approach builds a model that closely represents the observed climate using statistical relationships between observations and simulations. It remains a widely used approach due to its relatively simple bias correction process and low computational cost (Mehrotra and Sharma (2015); Cannon (2018); Tabari et al. (2021)). In line with these attempts, to simplify this process, various software toolkits have been developed. Cannon (2016) developed an R package supporting multiple bias correction techniques, from simple quantile mapping to advanced methods that correct multivariate relationships between surface variables. Mehrotra et al. (2018) developed an R package that supports bias correction approaches for multiple surface variables across different time scales, focusing on low-frequency precipitation variability using a nested approach. While these packages simplify the bias correction process, enabling users to easily correct variables and analyze model performance, they can present challenges due to artifacts in downscaled signals and assumptions of time invariance when correcting output variables directly (Rahimi et al., 2024).

Pre-downscaling bias correction, on the other hand, involves adjusting the GCM's climatological statistics towards reanalysis data to remove biases from the GCM datasets. Several approaches for bias correction have been employed, ranging from simple scaling (Xu and Yang (2012); Bruyere et al. (2014)) to more complex techniques that attempt to mimic observed multi-scale relationships in simulations (Rocheta et al. (2017); Kim et al. (2021); Kim et al. (2023a)). These methods correct RCM input boundary conditions and have been shown to improve the accuracy of output variables, particularly for extreme events (Kim et al., 2023a). Furthermore, Kim et al. (2023b) demonstrated that multivariate bias-corrected boundary conditions better represent compound events where multiple extremes occur simultaneously at the same location. Although this approach, while effective, may disrupt the physical consistency between variables in the GCM boundary conditions when correcting statistics of the simulated variables toward those of reanalysis data, the RCM will re-establish its own internal relationships between variables in the downscaled outputs, which are physically consistent and interpretable (Rahimi et al., 2024).

A recent study developed a multivariate bias correction approach at the sub-daily time scale to correct the rainfall diurnal cycle, which is crucial for simulating extreme events. They used quantile mapping (QM) to adjust the probability distribution of the scale factor, highlighting that sub-daily correction of the RCM input boundary conditions can improve diurnal precipitation patterns and other statistics compared with daily correction (Kim et al., 2023c).

In brief, pre-downscaling bias correction shows improved performance, particularly for extreme events, while ensuring the physical and dynamical consistency of RCM outputs. Despite these advantages, this bias correction process requires large



65 matrices and complex mathematical formulations, making it challenging for users to apply and limiting the benefits of
correcting atmospheric variables before downscaling. To resolve this issue, a previous study developed a Python package
that corrects full atmospheric fields at a sub-daily time scale before generating RCM input boundary conditions, focusing on
the historical period (Kim et al., 2023d). However, it was limited in application due to its Fortran-based script, which
consumed significant memory and storage, and fixed input format, which needs pre-processing that requires users to fairly
70 advanced programming skills.

This study focuses on the sub-daily multivariate bias correction of GCM simulations before dynamical downscaling to
address these issues, making the software applicable to most GCMs for simulating future climate and maximizing the
capabilities of bias correction.

75 This study developed a Python package, Sub-Daily Multivariate Bias Correction (SDMBC) v2 for future projections, which
corrects the full atmospheric fields and sea surface temperature of GCM datasets for both historical and future climate. It
supports high-performance computing, enabling parallel and efficient bias correction using several recently published
packages. It includes several bias correction approaches at multiple time scales, from sub-daily to yearly, as proposed by
Kim et al. (2023c). The package is primarily written in Python for efficiency in processing multiple input files, with the core
bias correction process remaining in Fortran due to its superior numerical calculation capabilities.

80 This paper describes the updated software package that simplifies the bias correction process. The paper is organized as
follows: Section 2 describes the bias correction approaches, Section 3 provides general details of implementing the bias
correction method in the Python package, Section 4 presents the results, and Section 5 concludes the study.

2. Bias correction approaches

A recent study developed a sub-daily multivariate bias correction approach to address the limitation of RCMs in reproducing
85 observed sub-daily rainfall intensities, particularly the diurnal cycle of precipitation (Kim et al., 2023c). This approach
combines QM and a multivariate bias correction method to adjust biases in the distributions at a sub-daily time scale, as well
as the inter-variable relationships among atmospheric variables at multiple time scales before dynamical downscaling,
aiming to enhance the simulation of extreme events and the diurnal precipitation cycle within the RCM domain. Users can
define the statistical attributes that should be corrected from: mean, standard deviation, and dependence attributes, lag1 auto-
90 and lag0 cross-correlation. The input variables are corrected at multiple time scales using a nesting approach, and the bias
correction processes are repeated a predefined number of times. The nesting approach, which corrects temporal persistence
as a form of the weighting factors, has shown improvement in the simulation of extreme events (Johnson and Sharma, 2012),
and a total number of iterations has been set to one as a default to avoid overcorrecting that can occur during the bias
correction process (Mehrotra and Sharma, 2012). More information on this approach can be found in Kim et al. (2023c). To
95 evaluate the bias correction techniques employed in this study, two time periods were selected. For calibration, a 31-year
sample spanning from 1959 to 1989 was chosen from both the GCM and observed data to compute the bias correction



factors. These factors were then applied to data from a separate period for validation, 1990 to 2020, to assess whether the bias correction performs effectively when applied outside the calibration sample.

3. Bias correction of historical and future simulation package, SDMBCv2

100 The SDMBCv2 developed here represents the next generation of SDMBC, providing bias-corrected atmospheric variables for both future and historical periods. This section outlines the application of bias correction methods to the instantaneous input datasets, encompassing interpolation and reformation (see Figure 1). It details the input requirements, interpolation processes, implementation of bias corrections, and the output formats available in the package.

3.1 User-defined input information for interpolation

105 Before applying bias correction, users first need to interpolate the reanalysis dataset to match the spatial and temporal resolution of the target GCM. This preprocessing step ensures that both datasets share a consistent grid structure, facilitating seamless integration. The software developed in this study automates this process through horizontal and vertical interpolation, with input and output specifications managed via a configuration file ('config_interp.yaml').

110 The interpolation procedure involves resampling key atmospheric variables—including specific humidity (q , kg/kg), temperature (t , K), zonal wind (u , m/s), meridional wind (v , m/s), and sea surface temperature (sst)—which define the lateral and lower boundary conditions of the model. Here 6-hourly instantaneous values are used.

115 For horizontal interpolation, the software employs bilinear or conservative remapping techniques, depending on the variable, utilizing the xESMF library and Climate Data Operators (CDO) for high-precision grid transformations. Vertical interpolation is performed by aligning the input dataset's coordinate system with the target model's levels, incorporating geopotential height information to ensure consistency. To optimize performance and scalability, the script is designed to handle large datasets efficiently using Dask for parallel processing. This implementation enhances computational efficiency while maintaining accuracy, ensuring the interpolated observations are well-aligned with the GCM for subsequent bias correction and climate simulations.

120 Interpolation is necessary for the reanalysis dataset during both calibration and validation periods to enable proper bias correction functioning.

3.2 Overview of bias correction for a historical period

Once the input datasets have been accurately interpolated, the next step involves applying bias correction to the GCM variables. This process ensures that the climatological statistics of the GCM data are aligned with those of the reanalysis dataset, improving the reliability of the corrected outputs. The bias correction procedure consists of multiple key steps and 125 follows an approach similar to that implemented in the SDMBC package. A concise overview of this methodology is



provided in the following section, with further technical details available in the SDMBC documentation and Kim et al. (2023d).

3.2.1 Reanalysis and GCM attributes calculation

Prior to bias correction, both reanalysis and GCM 6-hourly instantaneous datasets are aggregated to a daily time scale by 130 computing the mean of the 6-hourly values. During this process, sub-daily fractions (SF)—representing the contribution of each 6-hour value to the daily average—are calculated and stored for subsequent use in downscaling bias-corrected daily variables back to their original 6-hourly resolution. The software includes a QM approach to correct scaling factors, adjusting the distribution of GCM outputs to align with the cumulative distribution function (CDF) of the observed dataset. Users can specify the use of sub-daily bias correction in the configuration file, enabling this adjustment process. 135 Key statistical attributes are computed using a centered moving window approach (Sharma and Lall, 1999) for both observed and GCM variables using the resampled daily time series. A detailed description of the transformation function applied in this study is provided in Kim et al. (2023c).

3.2.2 Correction of GCM attributes

To correct the raw daily GCM variables, we first adjust their climatological mean and standard deviation. This is achieved 140 by replacing the raw mean with the reanalysis mean, then normalizing by the raw standard deviation and rescaling with the reanalysis standard deviation. The transformed time series are subsequently standardized, after which adjustments are applied to preserve both auto- and cross-correlation structures using a simplified multivariate autoregressive model (Salas, 1980).

Following these adjustments, the bias-corrected daily series are aggregated to longer temporal scales, including monthly, and 145 seasonal periods. The corrected values are then rescaled to maintain consistency in mean and standard deviation. Additionally, the bias-corrected variables are integrated into a hierarchical nesting framework (Kim et al., 2023a), where daily GCM data incorporate bias correction effects observed at coarser temporal scales. This approach ensures that persistence characteristics are retained across time scales. The bias-corrected values at multiple time scales serve as weighting factors for the uncorrected daily GCM data, as outlined by Srikanthan and Pegram (2009). These bias correction 150 steps are iteratively applied in a recursive manner, with the total number of iterations defined by the user. In this study, we perform one iteration, as noted in Section 2.

Finally, the bias-corrected daily series are rescaled to a 6-hourly resolution using the sub-daily fractions calculated previously. A detailed description of these procedures is provided in Figure 1.

3.3. Overview of bias correction for a future projection

155 The next step involves applying bias correction parameters to future GCM variables. This process aims to align the climatological statistics of the future GCM data with those of the differences between GCM and observed datasets in the



current period. The following sections provide an overview of the bias correction methodology applied to future GCM data, with further details available in the relevant documentation.

3.3.1 Calculation of future GCM attributes

160 Future GCM 6-hourly instantaneous datasets are first aggregated to a daily time scale by averaging the 6-hourly values, following the same approach used for historical data. Users can enable sub-daily bias correction for future periods through the configuration file, allowing for refined adjustments. Key statistical attributes—including climatological mean, standard deviation, lag-1 auto-correlation, and lag-0 cross-correlation—are then computed for future GCM variables across multiple time scales, ranging from daily to seasonal periods.

165 3.3.2 Correction of future GCM attributes

Bias correction parameters derived from the historical period are applied to future simulations. For sub-daily correction, the same QM approach used for historical data is implemented. This involves determining the difference between the CDFs of reanalysis and current-climate GCM data and using this difference to correct future GCM values under the assumption that biases present in the current period will persist in future simulations. The correction process begins by correcting the future 170 GCM climatological mean, achieved by subtracting the difference between the current GCM and reanalysis climatological means. The standard deviation is then corrected by scaling it according to the ratio of the reanalysis standard deviation to the current GCM standard deviation. Additionally, auto- and cross-correlation coefficients are adjusted to preserve observed dependencies within nested and multivariate bias correction frameworks. The bias correction parameters derived from historical periods can be applied recursively, with the total number of iterations defined by users. Further details on these 175 procedures are available in Kim et al. (2023d).

3.4 Output data information

The bias-corrected GCM datasets used for generating RCM input boundaries include four three-dimensional atmospheric variables at each vertical level, along with sea surface temperature. The package allows these outputs to be automatically reformatted to match the original file structure, provided users specify this option in the configuration file. As a result, the 180 bias-corrected outputs retain the same NetCDF format as the original GCM data, eliminating the need for additional processing. This ensures seamless integration into RCM workflows, allowing users to employ the same scripts or procedures previously used with raw GCM inputs.

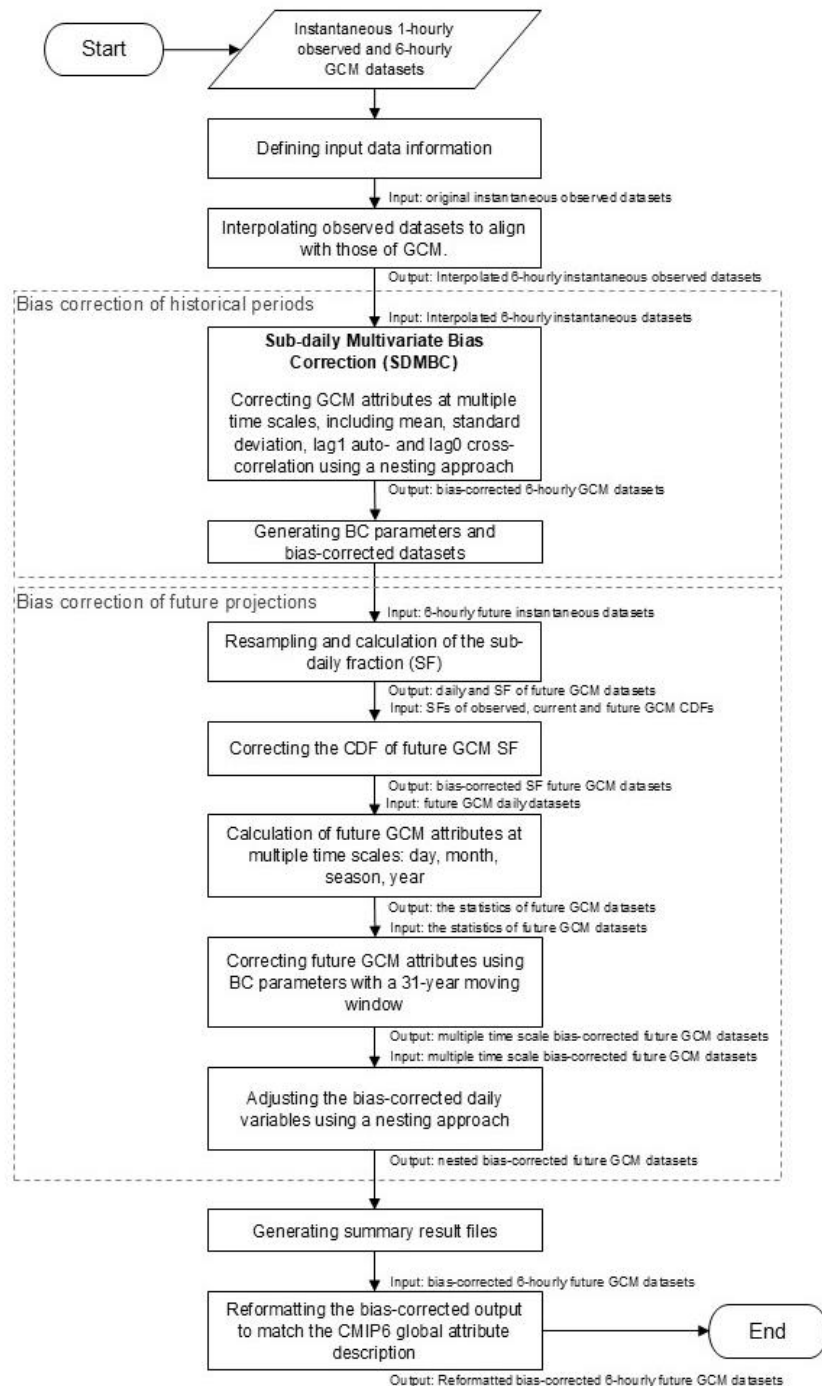


Figure 1 A schematic diagram of SDMBCv2.



185 4. Experiment design

This section presents the datasets and experimental design employed in the study, as well as the evaluation metrics used.

4.1 Datasets and experimental setup

To evaluate the performance of SDMBCv2, we used the Australian Community Climate and Earth System Simulator Earth System Model Version 1.5 (ACCESS-ESM1.5) (Ziehn et al., 2020) as the source GCM. ACCESS-ESM1.5 operates on an 190 N96 Gaussian grid with a spatial resolution of approximately 1.875° longitude $\times 1.25^\circ$ latitude and includes 38 vertical levels. ERA5, the fifth-generation reanalysis dataset from the European Centre for Medium-Range Weather Forecasts (Hersbach et al., 2020), was used as the reference. It provides a horizontal resolution of approximately 31 km and includes 37 pressure levels.

Bias correction was applied to key variables required for regional climate model boundary conditions: specific humidity q (kg/kg), temperature ta (K), zonal wind u (m/s), and meridional wind v (m/s), and sea surface temperature sst (K).

The SDMBCv2 package first harmonized the spatial and temporal resolutions between the GCM and ERA5 datasets through a two-step interpolation process: conservative remapping was used for specific humidity, while bilinear interpolation was applied to the remaining variables. Vertical interpolation was performed to align the ERA5 levels with the vertical structure of ACCESS-ESM1.5. SST regridding was also necessary to ensure consistency with the GCM grid.

200 Both datasets were preprocessed to ensure identical spatiotemporal dimensions prior to bias correction. This alignment ensures that corrected GCM variables can be seamlessly used as input boundary conditions for regional climate models. It is important to note that all other model variables remain unchanged and that boundary conditions are established only after bias correction is applied.

The bias correction process was conducted over two distinct periods: a 31-year calibration period (1959–1989) and a 31-year 205 validation period (1990–2020).

4.2 Performance assessment

The impact of bias correction was evaluated using two primary statistical metrics: Mean Absolute Error (MAE) and Bias. The MAE quantifies the average absolute difference between model simulations and observed values across all grid cells and 210 is defined as:

$$MAE = \frac{1}{N} \sum_{n=1}^N |X_n^{mod} - X_n^{obs}|, \quad (1)$$

where N is the total number of grid cells, X_n^{mod} and X_n^{obs} represent the climatological values from the GCM and observed datasets at each grid cell, respectively.

Bias, representing the systematic deviation between model simulations and observations, is calculated as:



215

$$Bias = \frac{1}{N} \sum_{n=1}^N (X_n^{mod} - X_n^{obs}). \quad (2)$$

Bias values are computed individually for each grid cell.

Additionally, the Kolmogorov-Smirnov (K-S) test was employed to statistically evaluate the similarity between the probability distributions of model simulations and observations. The K-S test measures the maximum absolute difference (L) between the cumulative distribution functions (CDFs) of the model ($F_g(x)$) and observed ($F_o(x)$) data:

220

$$L = \max_x |F_g(x) - F_o(x)|. \quad (3)$$

The null hypothesis of the K-S test is that both samples originate from populations with identical distributions. The null hypothesis is rejected if the calculated test statistic (L) exceeds the critical value ($L_{critical} = c(\alpha) \sqrt{\frac{n_1+n_2}{n_1 n_2}}$), where n_1 and n_2 denote the sample sizes of the model and observational datasets, respectively, and $c(\alpha)$ is a constant determined by the significance level α . Alternatively, rejection occurs if the p-value is less than 0.05.

225

5. Results

This section presents an evaluation of the bias correction performance across multiple time scales. We assess the correction performance by comparing key climatological statistics during both the calibration and validation periods against reanalysis datasets. Although the SDMBCv2 package produces bias-corrected outputs across full vertical levels and spatial domains, 230 this study focuses on selected grid cells for vertical analysis and lower atmospheric levels for horizontal. The evaluation is based on several diagnostic metrics, including the climatological mean, standard deviation, lag-1 autocorrelation, multivariate dependence, and sub-daily distribution characteristics.

5.1 Bias-corrected GCM datasets: calibration

235 This section assesses the performance of the bias correction during the calibration period. The primary goal is to evaluate whether the SDMBCv2 framework reduces biases in key statistical properties across various time scales.

Figure 2 presents bias maps of the seasonal statistics used to evaluate seasonal variability in SST, comparing uncorrected and bias-corrected GCM outputs against ERA5 for the calibration period. The upper panels display the biases in the raw GCM, while the lower panels illustrate the results after bias correction with SDMBCv2.

240 The raw GCM exhibits a strong negative bias in the seasonal mean, particularly in the Southern Ocean, with a domain-averaged mean absolute bias of 0.9°C. The standard deviation is also notably overestimated in several key regions, including the tropical Atlantic and Pacific, with an average bias of 0.4°C. Biases in lag-1 autocorrelation are generally lower in



magnitude but still evident in convectively active regions, with localized deviations exceeding 0.3. Such errors can influence the representation of SST persistence and feedback in coupled models.

245 In contrast, the bias-corrected SST fields show near-zero deviations across all three metrics indicating good agreement with the reference.

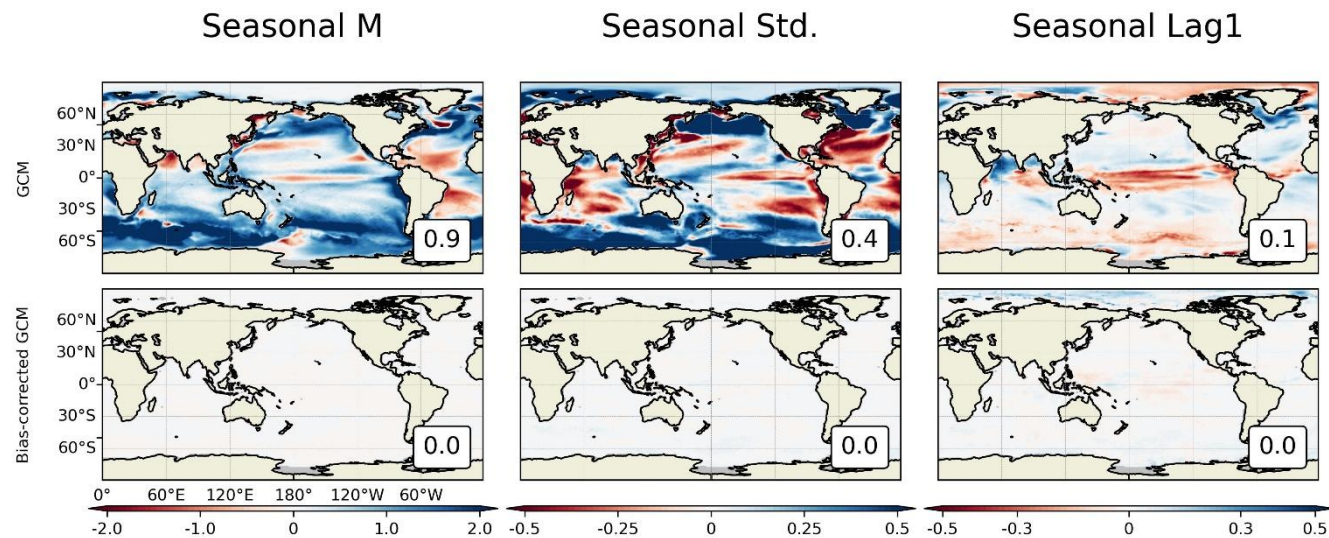


Figure 2 Seasonal bias map of sea surface temperature (SST) for both GCM and bias-corrected data in calibration periods from 1959 to 1989. The number at the bottom right shows the mean absolute error.

250

Figure 3 presents bias maps of the climatological mean, comparing ERA5 to both the uncorrected and bias-corrected GCM outputs for three atmospheric variables at the lowest model level on a daily time scale across the entire domain.

The left panels reveal substantial biases in the original GCM outputs, including an obvious underestimation of wind speed, widespread warm biases in air temperature, and excessive specific humidity, particularly across the tropics and mid-latitudes.

255

These systematic errors can propagate through regional climate models, degrading their performance. For instance, underestimated wind speed may suppress key processes like moisture transport and convective uplift, while overestimated temperature and humidity can amplify convective feedback, potentially distorting projections of extreme events such as heatwaves or intense precipitation.

In contrast, the right panels demonstrate the effectiveness of SDMBCv2 in eliminating these biases. The post-correction fields show negligible residual errors across all three variables.

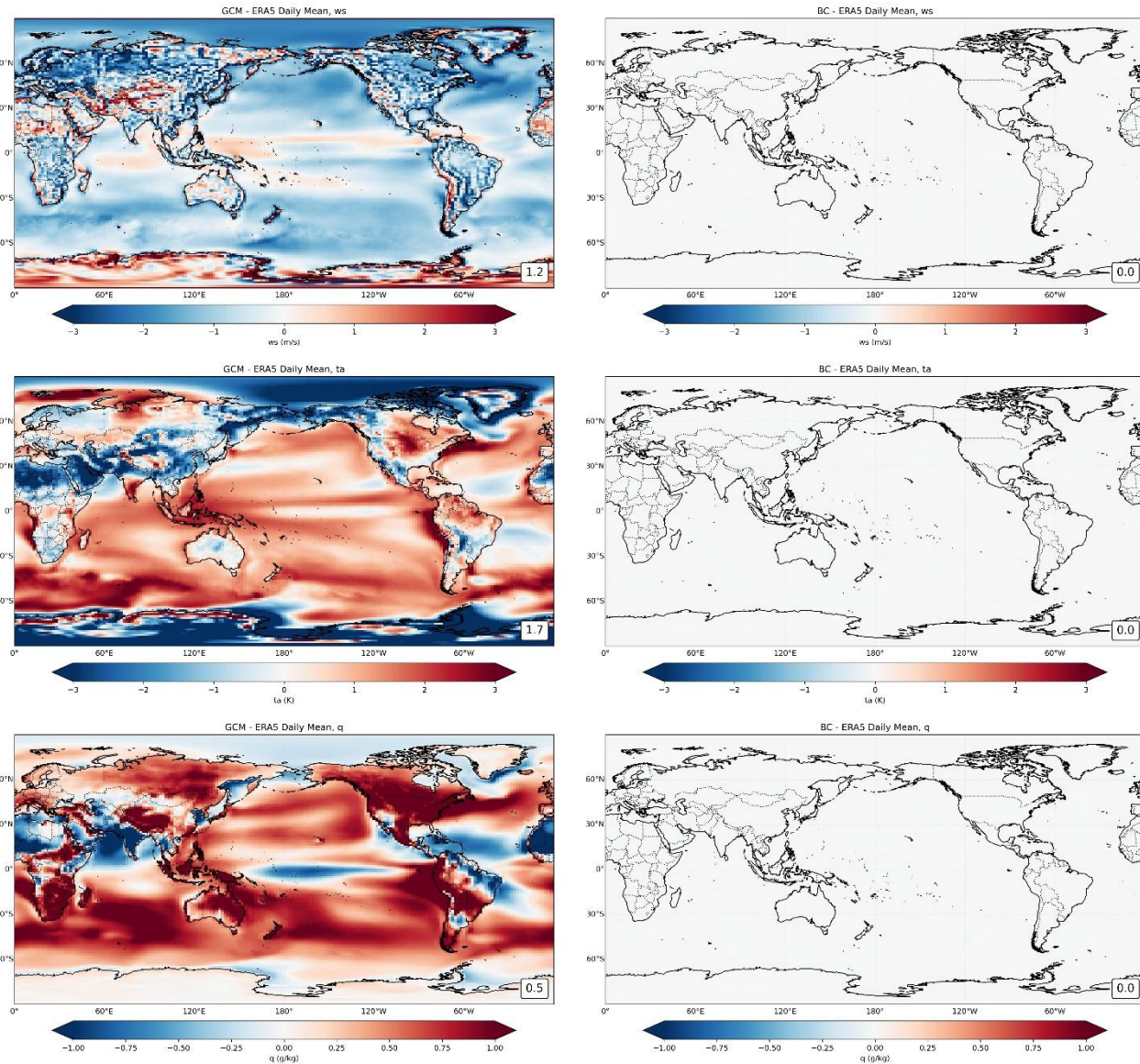


Figure 3 Climatological mean bias maps comparing ERA5 with GCM outputs before (left panels) and after (right panels) bias correction (BC), evaluated at the lowest model level on a daily time scale for the calibration period (1959–1989). The panels show results for wind speed (ws), air temperature (ta), and specific humidity (q). The number at the bottom right shows the mean absolute error.

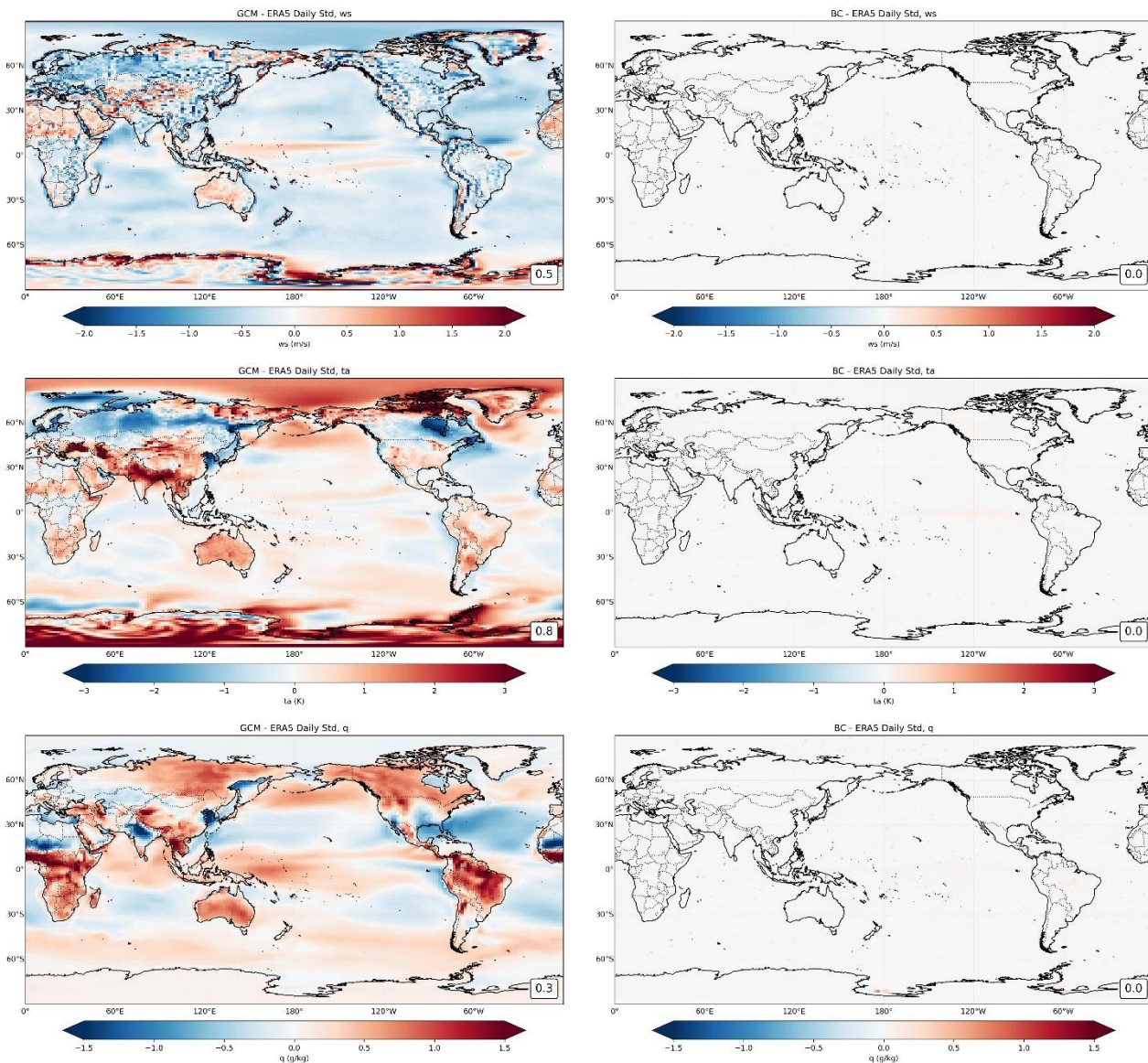
265

Figure 4 presents bias maps of the standard deviation, corresponding to the climatological mean comparisons shown in
270 Figure 3. These maps illustrate how the SDMBC framework improves the representation of daily variability in key atmospheric variables. The results show that the uncorrected GCM exhibits notable deficiencies. Wind speed variability is underestimated, particularly across mid-latitude regions, potentially suppressing the simulation of wind-driven processes



275

such as turbulence, vertical mixing, and mesoscale circulation. Specific humidity also shows strong positive biases in the tropics, indicating an overrepresentation of moisture variability. Such biases can exaggerate convective activity and lead to unrealistic intensification of extreme rainfall events in downscaling applications. On the other hand, biases in variability are substantially reduced after bias correction across most regions, with near-zero deviations in wind speed, temperature, and specific humidity.



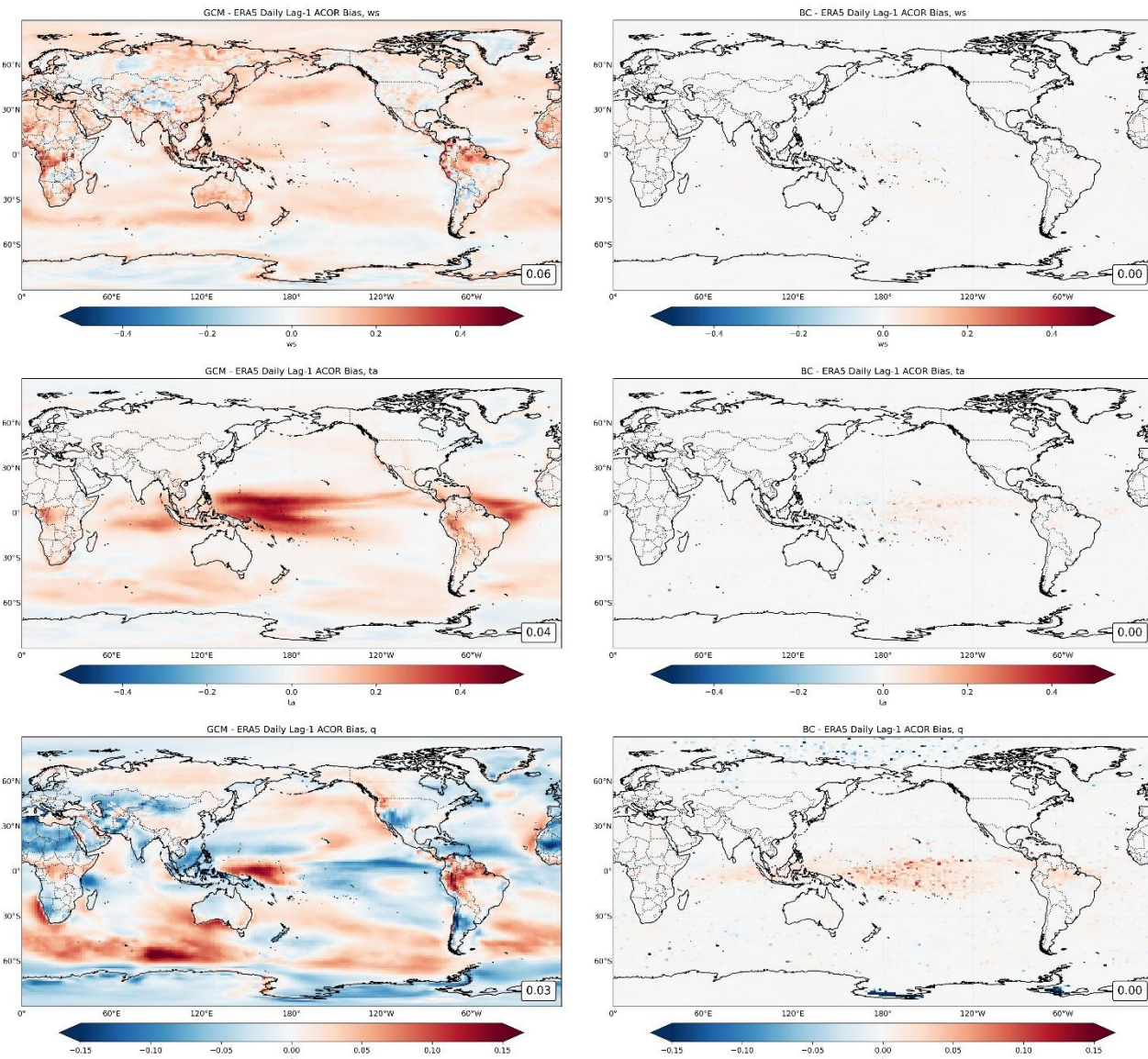
280

Figure 4 As in Figure 3, but for standard deviation



Figure 5 compares lag-1 autocorrelation between the uncorrected GCM and the bias-corrected GCM at a daily timescale. The results indicate that the uncorrected GCM displays widespread positive biases in lag-1 autocorrelation, especially for air 285 temperature over tropical regions and for specific humidity in convective zones. These positive biases indicate that the model overestimates short-term memory, potentially leading to an unrealistic persistence of extreme events such as prolonged heatwaves or wet spells. Conversely, positive biases in wind speed autocorrelation are also evident, suggesting that the model overrepresents the continuity of wind motion, which could influence the simulation of storms and large-scale circulation features.

290 Following bias correction, these spurious persistence patterns are largely removed. The corrected fields show near-zero biases across most regions, indicating that SDMBCv2 successfully adjusts not only the mean and variability but also the temporal correlation structure of atmospheric variables—an essential feature for improving the realism of climate simulations used in downscaling.



295

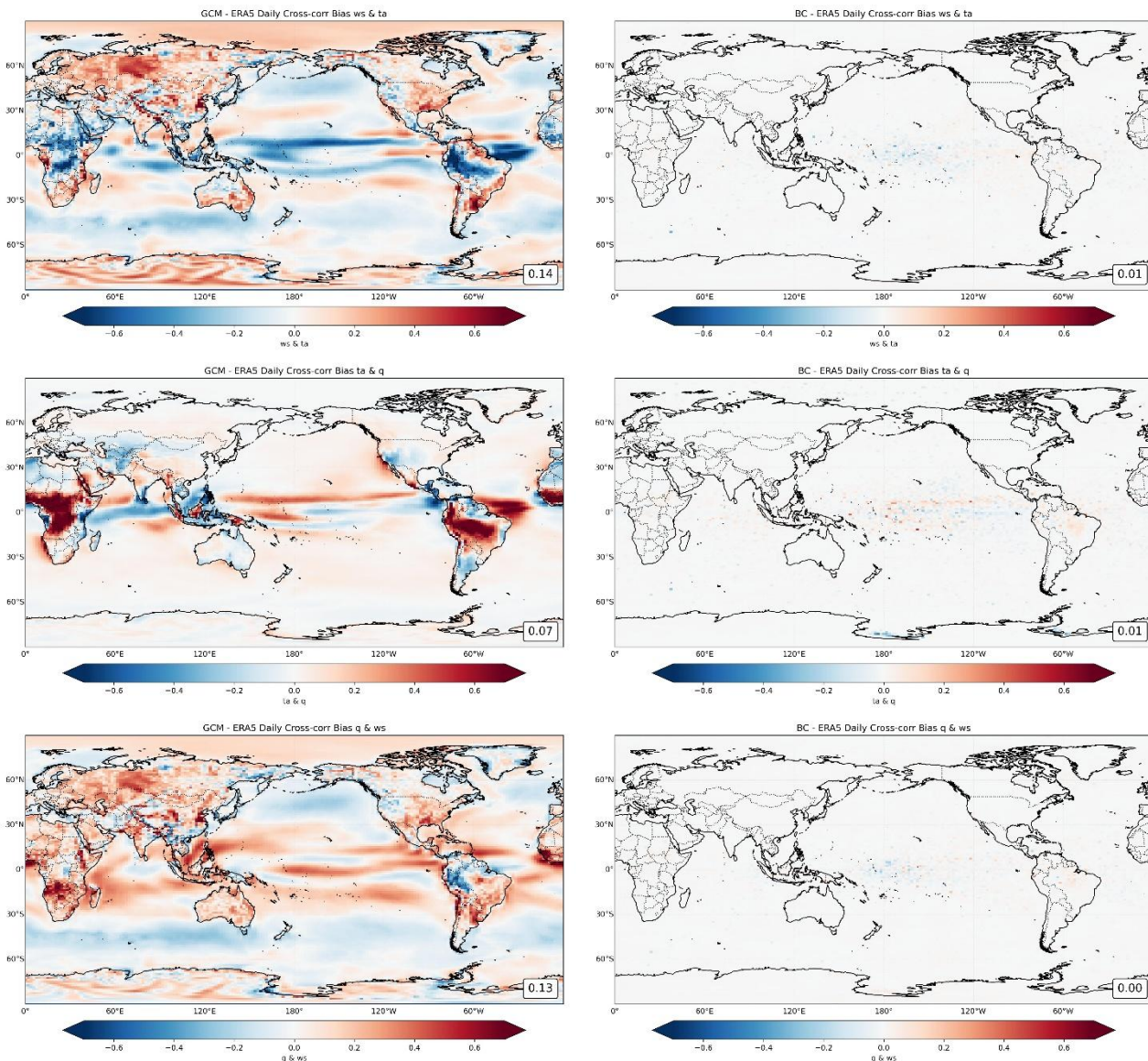
Figure 5 As in Figure 3, but for lag1 auto-correlation

Figure 6 presents bias maps for lag-0 cross-correlation, similar to Figure 3. The uncorrected GCM exhibits notable cross-correlation biases, particularly in regions influenced by deep convection and strong large-scale circulation. For example, a 300 positive bias in the cross-correlation between air temperature and specific humidity (ta & q) over tropical regions suggests an overestimated coupling between thermal and moisture fields. This could lead to exaggerated feedback in moist convection, ultimately distorting projections of heat stress and precipitation extremes. Similarly, the cross-correlations between wind



speed and temperature (ws & ta), and wind speed and specific humidity (ws & q), display substantial regional biases, which may degrade the representation of energy and moisture fluxes essential for storm development and atmospheric stability.

305 In contrast, the bias-corrected outputs demonstrate near-zero deviations across most regions, indicating that SDMBCv2 effectively restores realistic inter-variable relationships.



310 Figure 6 As in Figure 3, but for lag0 cross-correlation



Figure 7 presents scatter plots comparing observed values with both uncorrected and bias-corrected GCM outputs for key atmospheric variables across 24 vertical levels within the study domain. To ensure reliability, levels where specific humidity approaches zero—where statistical moments become unstable—were excluded from the analysis, following guidance from prior studies (Kim et al., 2023d).

315 The figure evaluates the impact of bias correction across multiple statistical measures: mean, standard deviation, lag1 auto-correlation, and lag0 cross-correlation, at different temporal scales, including daily, monthly, and seasonal. The results demonstrate a clear improvement following bias correction. Furthermore, the figure shows that the uncorrected GCM variables exhibit significant biases in inter-variable relationships, potentially leading to unrealistic atmospheric behavior.

320 These biases can distort essential physical interactions such as moisture transport, energy exchange, and convective processes, ultimately affecting the reliability of regional climate projections. In contrast, the bias-corrected GCM variables align well with observed data, with most points clustering near the 45-degree line.

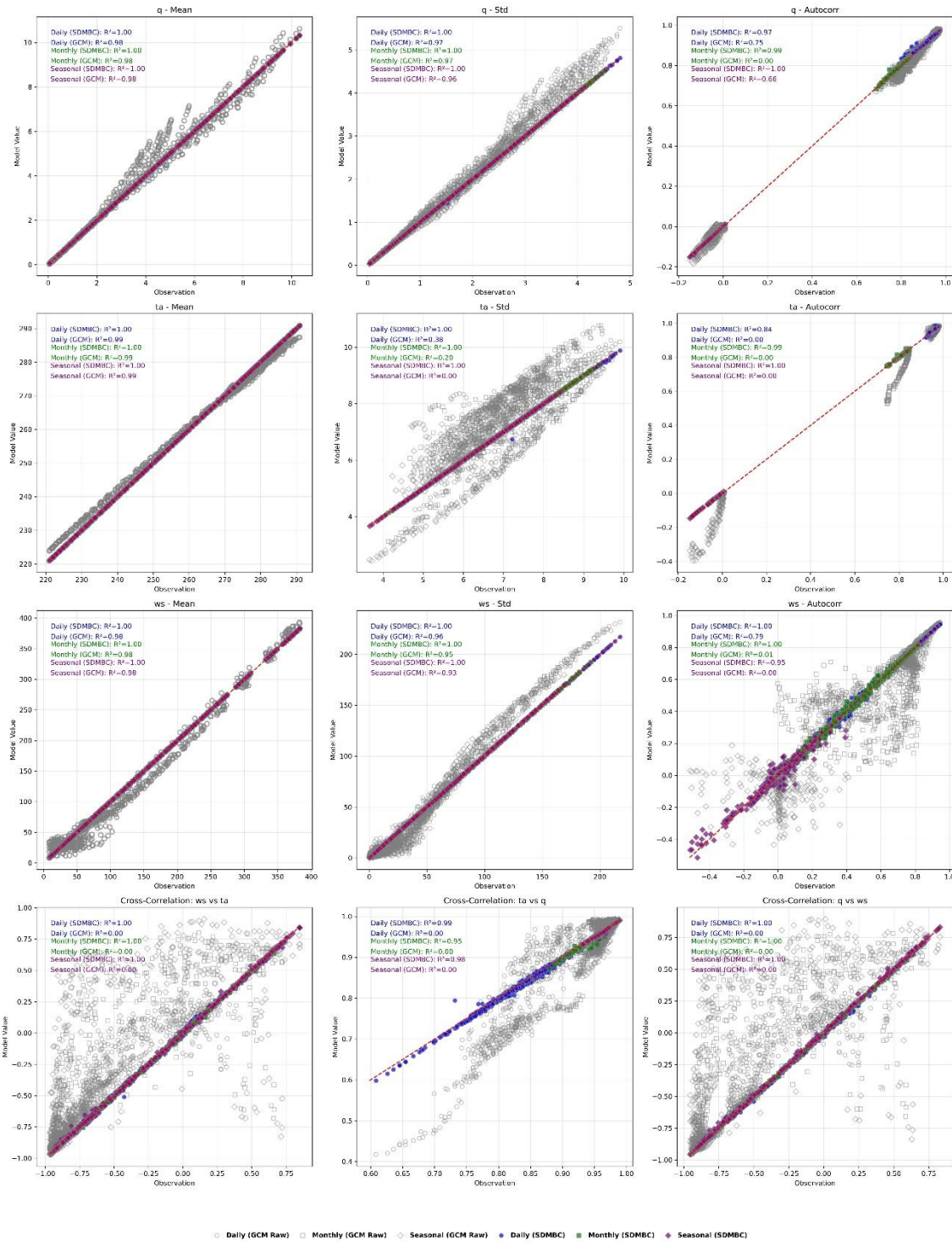


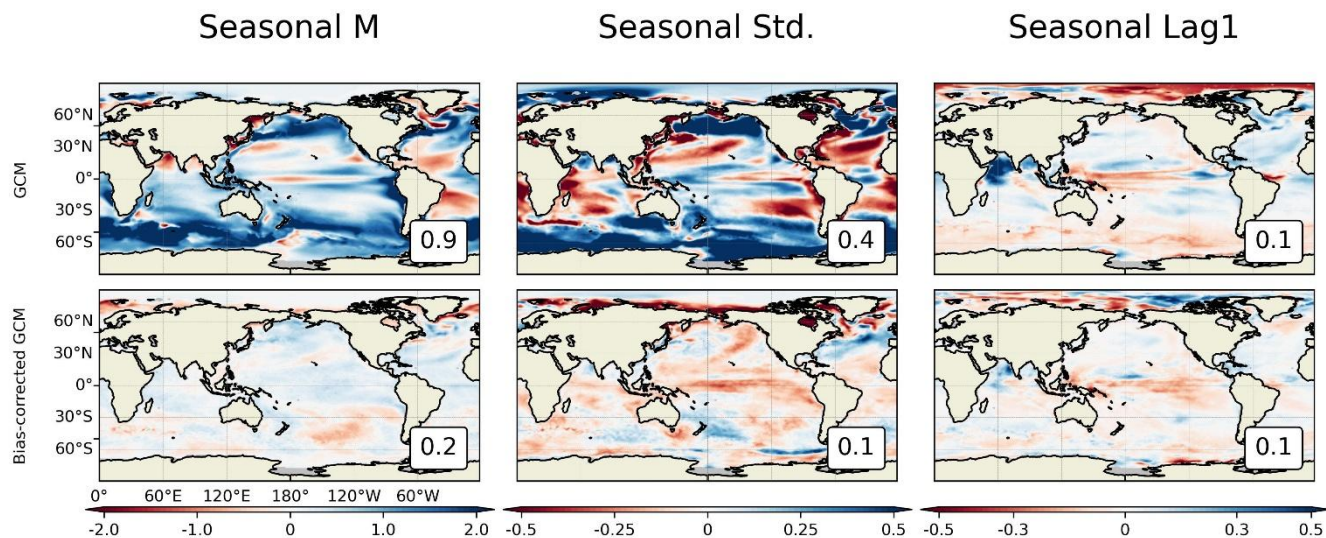
Figure 7 Scatter plot of atmospheric variables for climatological statistics across the vertical levels in the sampled domain in calibration periods from 1959 to 1989.



4.3 Bias-corrected GCM datasets: validation

This section evaluates the performance of the bias correction during the validation period (1990–2020), using the same spatial domain and variables applied during calibration. As in the calibration phase, the analysis includes sea surface temperature (SST) and key atmospheric variables, with selected grid cells examined to assess bias correction performance

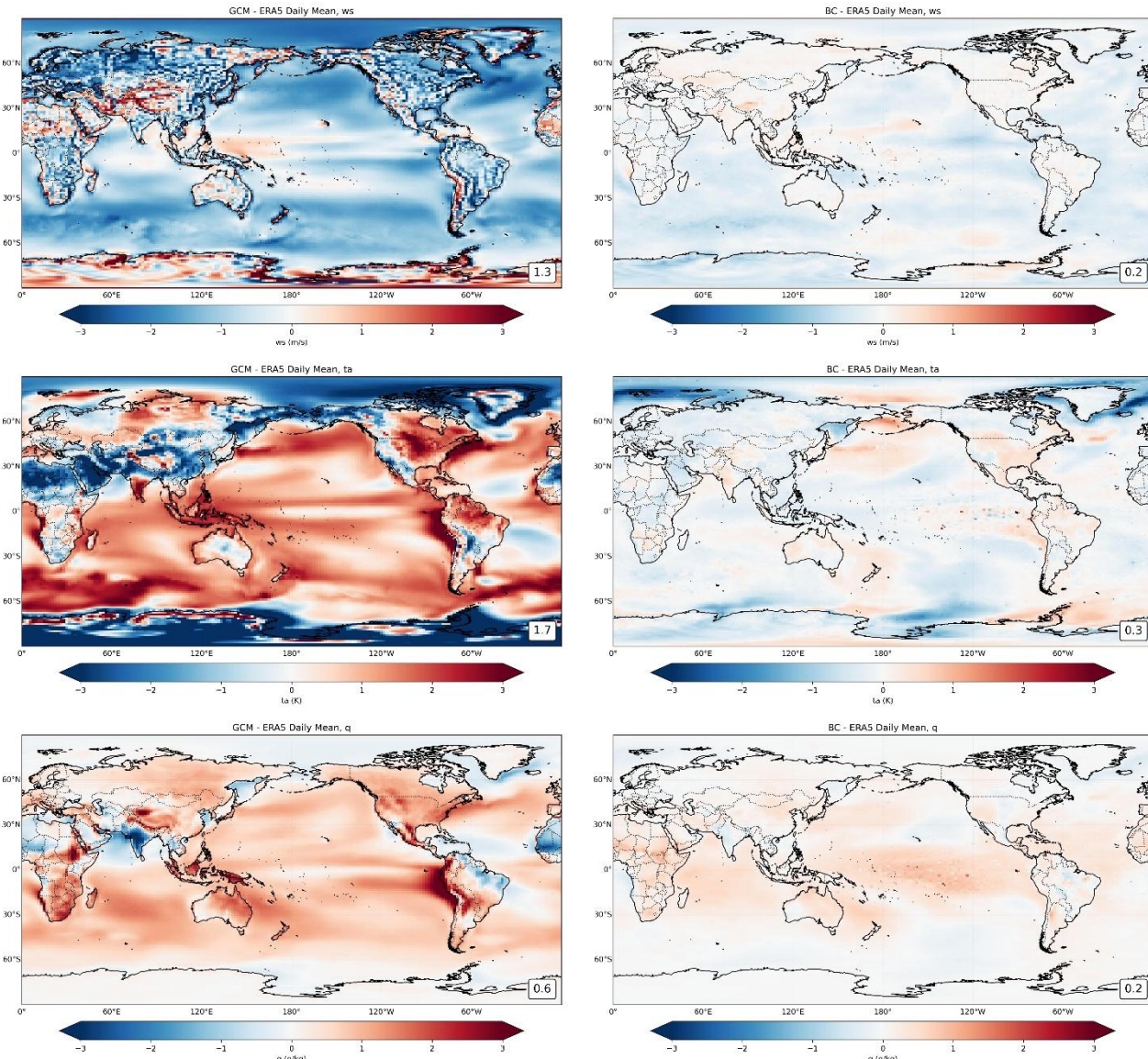
330 across vertical levels. The goal is to determine whether the improvements achieved during the calibration period are maintained over a distinct, independent time window and whether SDMBCv2 continues to reduce biases across multiple time scales and statistical dimensions.



335 **Figure 8 Seasonal bias map of sea surface temperature (SST) for both GCM and bias-corrected data in validation periods from 1990 to 2020. The number at the bottom right shows the mean absolute error.**

Figure 8 illustrates seasonal SST bias maps comparing uncorrected and bias-corrected GCM outputs against ERA5 during the validation period. The results show substantial biases in the seasonal mean of the uncorrected GCM, particularly in the Southern Ocean and equatorial Pacific, where the mean absolute bias reaches approximately 0.9°C. Following bias correction, these discrepancies are substantially reduced, with the global mean absolute bias decreasing to 0.2°C. Notable

340 improvements are observed in both high-latitude and tropical regions, where accurate SST representation is essential for resolving coupled ocean-atmosphere processes. The correction also reduces the bias in seasonal standard deviation from 0.4°C in the raw GCM to 0.1°C, with marked improvements in regions influenced by upwelling and in the North Atlantic. Furthermore, modest improvements are evident in seasonal lag-1 autocorrelation.



345

Figure 9 Bias maps of the climatological mean during the validation period (1990–2020), comparing uncorrected (GCM) and bias-corrected GCM outputs (BC) against ERA5 for three key atmospheric variables at the lowest model level. The left panels illustrate the raw GCM, while the right panels show the results after applying SDMBCv2. The number at the bottom right shows the mean absolute error.

350

Consistent with the calibration results, the uncorrected GCM from Figure 9 exhibits substantial biases in all three variables: wind speed (ws) is strongly underestimated, air temperature (ta) shows widespread warm biases and specific humidity (q) is excessively high in tropical and mid-latitude regions. On the other hand, following bias correction, mean biases are considerably reduced across all regions. The post-correction fields show small residual errors, with global mean absolute biases reduced from 1.3 to 0.2 m/s for wind speed, from 1.7 to 0.3 K for temperature, and from 0.6 to 0.2 g/kg for specific



355 humidity. These improvements confirm the robustness and generalizability of SDMBCv2 in reducing mean-state errors beyond the calibration period.

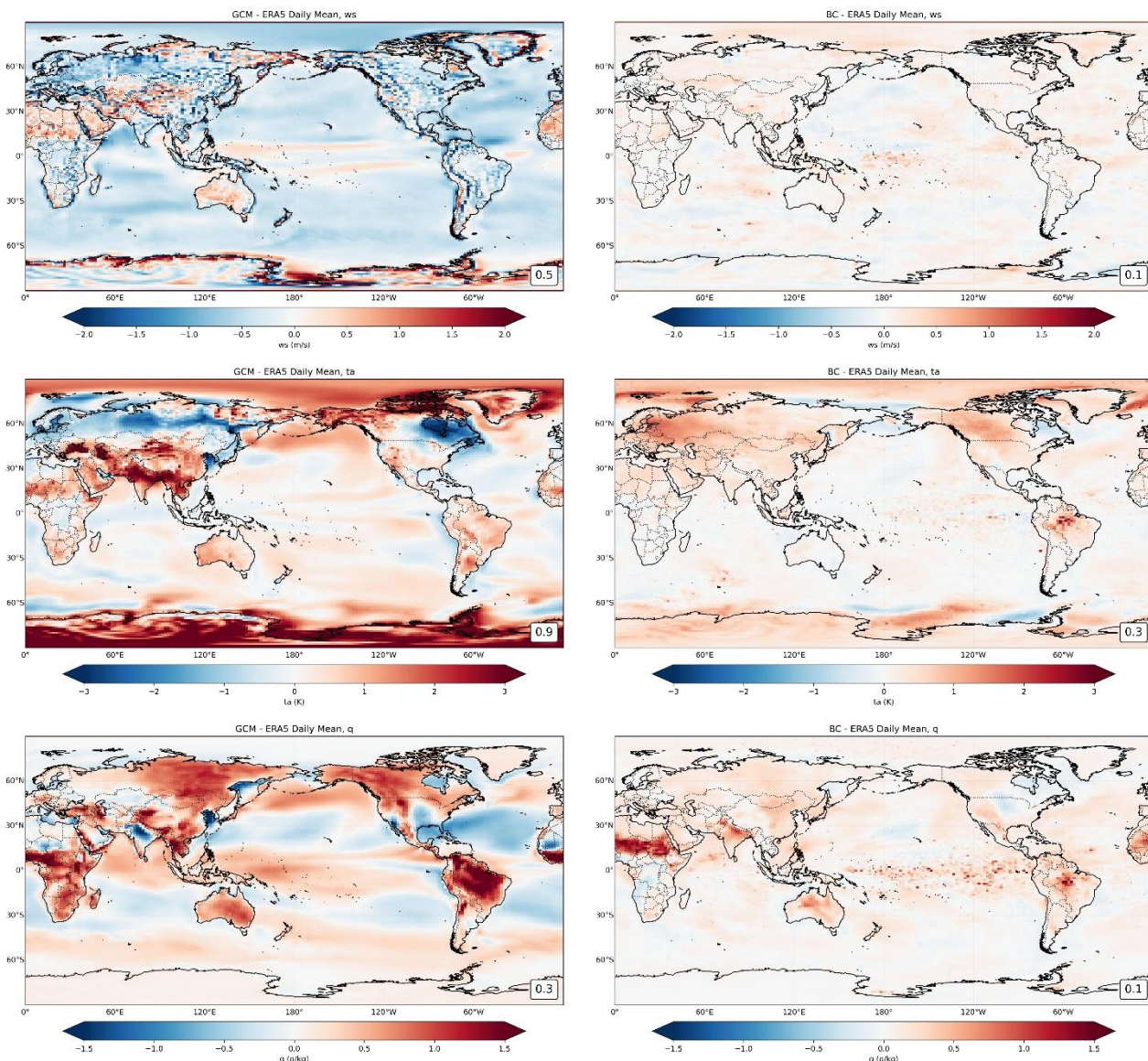


Figure 10 As in Figure 9, but for standard deviation

360 Figure 10 displays bias maps of the daily standard deviation during the validation period. The uncorrected GCM underestimates variability in the wind speed, with a global mean absolute bias of 0.5 m/s. Air temperature and specific humidity also exhibit widespread overestimation of variability, particularly in high-latitude and monsoon-influenced regions, with mean absolute biases of 0.9 K and 0.3 g/kg, respectively. On the other hand, after bias correction, variability biases are



substantially reduced across the domain. The corrected fields show global mean absolute biases of 0.1 m/s for wind speed,
 365 0.3 K for temperature, and 0.1 g/kg for specific humidity. Improvements are particularly evident in dynamically active
 regions, including the North Pacific, East Asia, and the Intertropical Convergence Zone, where realistic variability is
 essential for credible regional climate projections. However, some regions—such as parts of Africa—show a shift from
 negative to positive variability bias after correction; possible reasons for this are explored in the Discussion section. Overall,
 370 these results confirm the effectiveness of SDMBCv2 in adjusting not only mean-state conditions but also the amplitude of
 daily variability during an independent validation period.

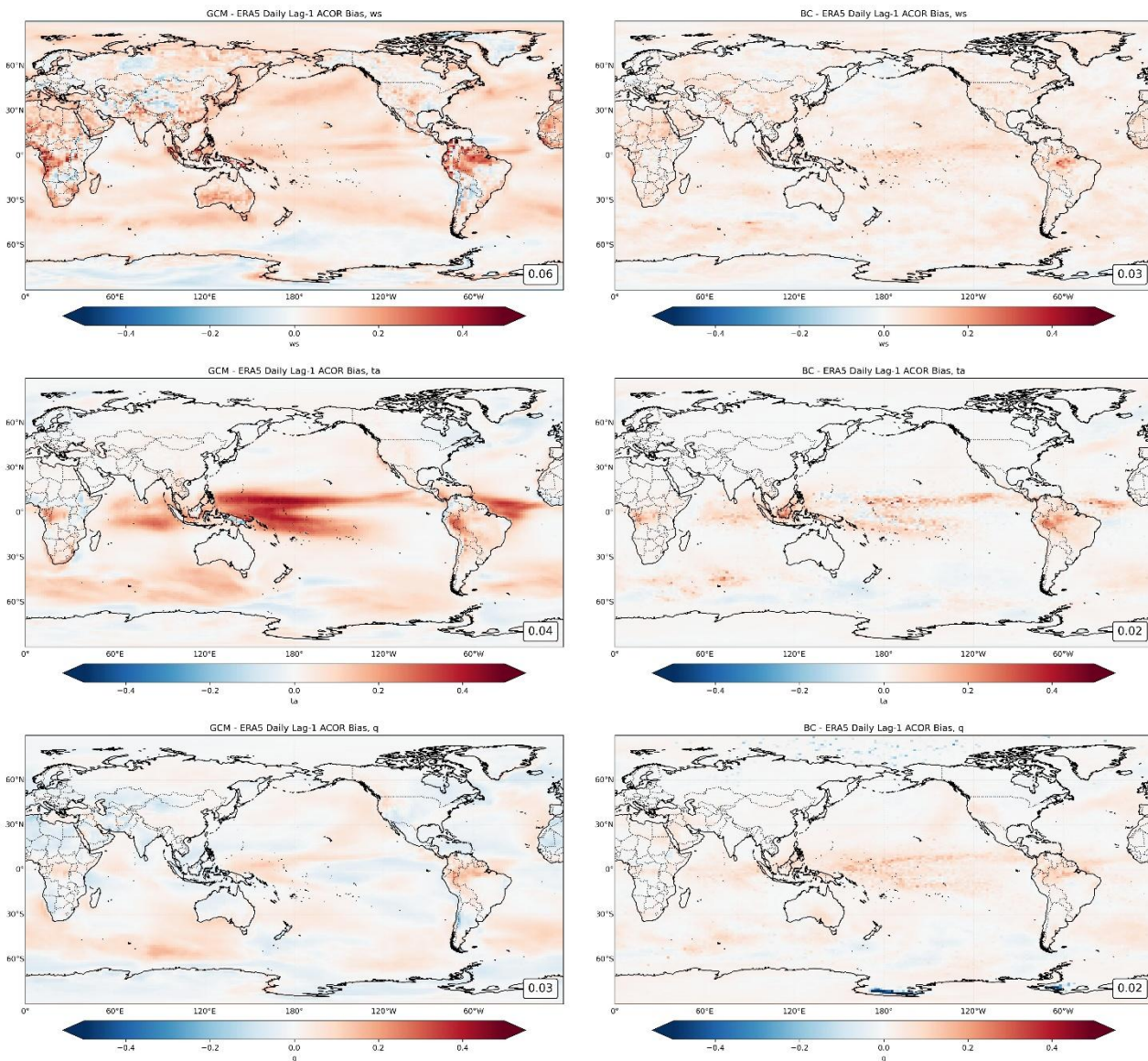


Figure 11 As in Figure 9, but for lag1 auto-correlation



Figure 11 presents bias maps of lag-1 autocorrelation for the validation period (1990–2020). Similar to the calibration period, the uncorrected GCM exhibits notable positive biases in temporal persistence, particularly for air temperature across
375 the tropical oceans and for specific humidity in convective regions. These elevated autocorrelations suggest an overestimation of short-term memory effects, which can lead to unrealistic persistence of heat or moisture-related extremes, such as multi-day heatwaves or prolonged wet periods. Following bias correction, these biases are largely mitigated. The corrected outputs exhibit small deviations across most regions, demonstrating that SDMBCv2 can adjust the temporal structure of atmospheric variables and preserve the observed persistence characteristics during the independent validation
380 period.

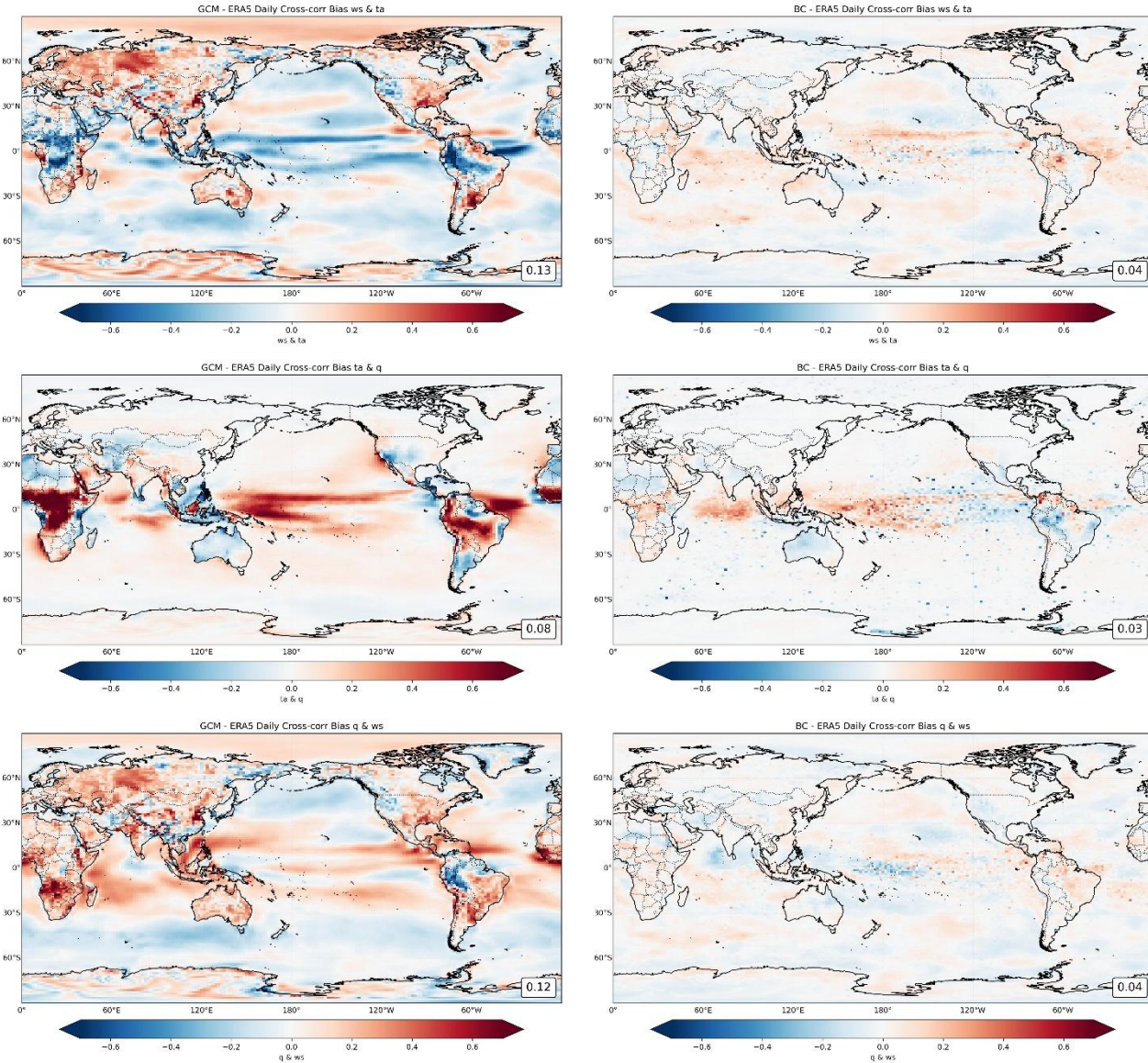


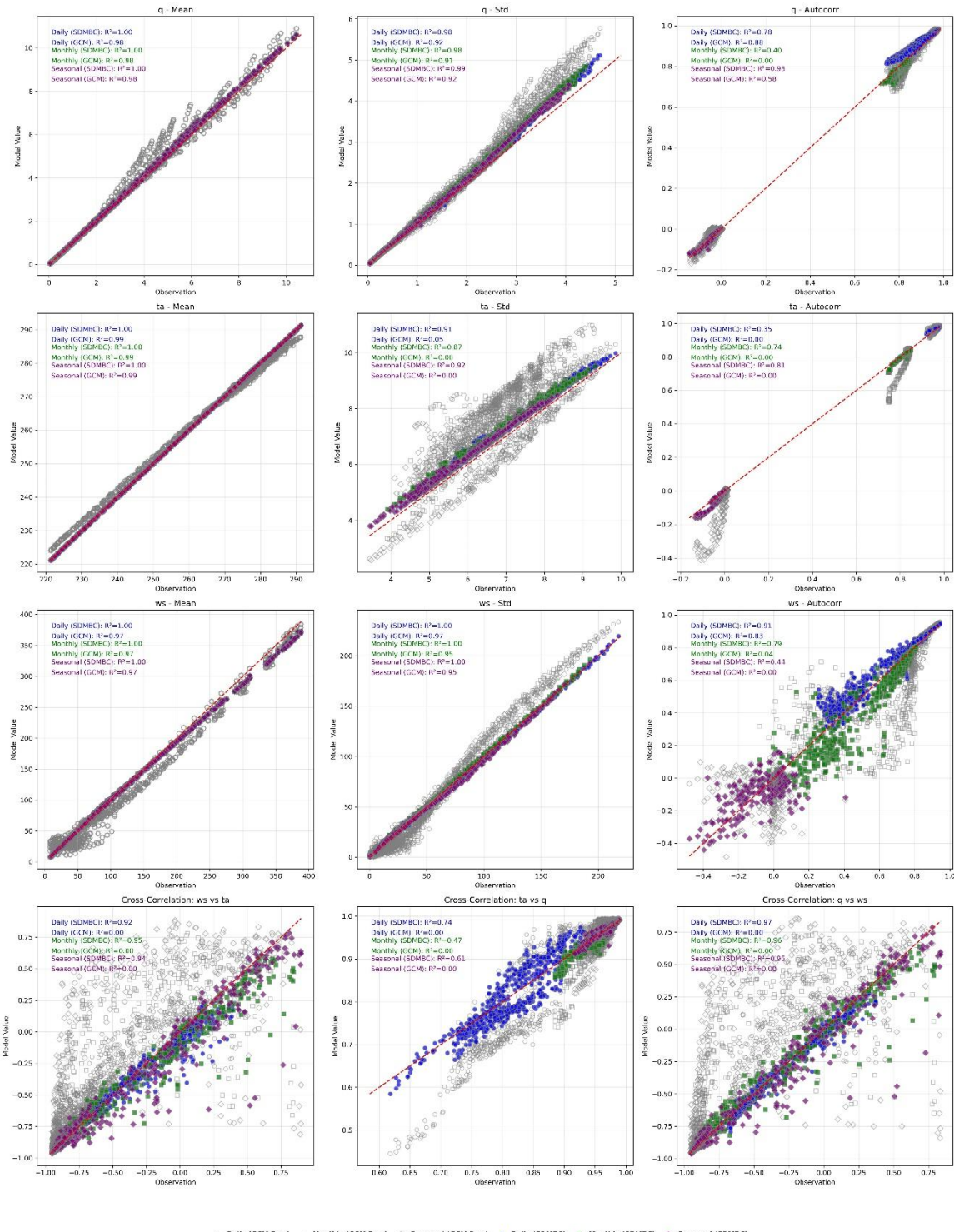
Figure 12 As in Figure 9, but for cross-correlation

Figure 12 shows bias maps of lag-0 cross-correlation for the validation period. In the uncorrected GCM, strong biases are evident in all variable pairings used in this study. These biases are most pronounced over tropical regions and convectively active zones, where the model tends to overestimate coupling strength. Such distortions can lead to unrealistic feedback in energy and moisture exchanges, ultimately affecting storm development, cloud formation, and precipitation processes.

385 After applying bias correction, cross-correlation biases are substantially reduced across most regions. The corrected fields exhibit only small bias, indicating that SDMBCv2 preserves key inter-variable dependencies and improves the physical



consistency of atmospheric states. These results confirm the framework's ability to correct not only univariate statistical
390 features but also the multivariate structure critical for realistic climate simulations.



○ Daily (GCM Raw) □ Monthly (GCM Raw) ◇ Seasonal (GCM Raw) ● Daily (SDMBC) ■ Monthly (SDMBC) ▲ Seasonal (SDMBC)

Figure 13 As in Figure 7, but for validation periods from 1990 to 2020.



395 Figure 13 presents scatter plots similar to those in Figure 7 but for the validation period (1990–2020). The results show that the bias-corrected GCM outputs consistently align more closely with observations across all metrics, exhibiting improved accuracy and reduced dispersion compared to the raw GCM data. The uncorrected GCM outputs display considerable biases in both univariate and multivariate statistics. In contrast, the SDMBCv2-corrected outputs exhibit strong clustering around the 1:1 reference line across most metrics and time scales, indicating a well-aligned statistical structure with observations.

400

Table 1 Percentage of grid cells passing the Kolmogorov–Smirnov (K–S) test at the 5% significance level, comparing the distribution of GCM outputs (uncorrected and SDMBC-corrected) to ERA5 observations at four 6-hourly time steps (00, 06, 12, 18) during the calibration and validation periods. Variables tested include wind speed (ws), air temperature (ta), and specific humidity (q).

		Calibration		Validation	
Time Interval	Variable	GCM	SDMBC	GCM	SDMBC
0	ws	73.34%	100.00%	54.59%	60.39%
0	ta	77.17%	100.00%	78.54%	81.40%
0	q	75.64%	100.00%	75.03%	79.93%
6	ws	62.31%	100.00%	47.01%	60.10%
6	ta	56.05%	100.00%	55.54%	81.31%
6	q	73.44%	100.00%	74.77%	80.60%
12	ws	51.57%	100.00%	38.60%	58.70%
12	ta	65.24%	100.00%	63.51%	81.47%
12	q	68.73%	100.00%	68.39%	80.59%
18	ws	74.09%	100.00%	54.68%	61.33%
18	ta	73.13%	100.00%	74.81%	81.64%
18	q	84.74%	100.00%	86.01%	80.48%

405

The results in Table 1 show a substantial improvement in distributional agreement with observations following bias correction. During the calibration period, 100% of sampled grid cells pass the K–S test for all variables and time steps after applying SDMBCv2, compared to notably lower rates in the raw GCM outputs. For example, raw GCM pass rates for wind speed range between 51–74%.

410

During the validation period, SDMBCv2 improves distributional performance across most variables and time steps. For air temperature (ta), the percentage of grid cells passing the K–S test exceeds 81% at all time steps after bias correction,



compared to 56–78% in the uncorrected GCM. Specific humidity (q) also shows consistent improvement at most times, with pass rates rising from 68–75% in the raw GCM to 80–81% following correction. However, at 18, the bias-corrected q pass rate (80.48%) is slightly lower than that of the uncorrected GCM (86.01%). This marginal reduction may reflect the 415 challenge of correcting humidity distributions in regions with high variability and complex diurnal moisture cycles, where even small shifts in distribution shape can affect K–S test sensitivity.

For wind speed (ws), SDMBCv2 improves the pass rate by 5–20 percentage points at each time step, though the corrected values (58–61%) remain modest compared to temperature and humidity.

4. Discussion and conclusion

420 This study evaluated the performance of the SDMBCv2 software, a Python package designed for sub-daily multivariate bias correction of GCM outputs used as boundary conditions for regional climate modeling. We focused on reducing systematic biases in atmospheric variables and SST across daily, monthly, and seasonal time scales. Our assessment involved comprehensive statistical evaluations against ERA5 reanalysis, using multiple metrics to test the consistency of corrected outputs during calibration (1959–1989) and an independent validation period (1990–2020).
425 The results consistently demonstrated that SDMBCv2 substantially reduces biases in GCM data, thereby improving the realism and reliability of simulated climate fields. Across all evaluated variables (wind speed, air temperature, and specific humidity) and statistical measures (mean, standard deviation, lag-1 autocorrelation, and lag-0 cross-correlation), the bias-corrected data exhibited marked improvement over the raw GCM simulations.

430 The analysis of climatological mean biases revealed that SDMBCv2 substantially corrects systematic errors in uncorrected GCM outputs. Large negative biases in wind speed, widespread warm biases in temperature, and excessive humidity across tropical and mid-latitude regions were minimized post-correction. These corrections have important implications, particularly for simulating climate extremes, where inaccuracies in atmospheric states can lead to unreliable projections of heatwaves, convective storms, and moisture-driven events.

435 SDMBCv2 also proved highly effective in adjusting variability metrics. Notably, the standard deviation biases were greatly reduced, reflecting an improved representation of temporal fluctuations essential for simulations of weather variability and associated phenomena, such as storm tracks, convective events, and boundary-layer processes. However, certain regions, notably parts of Africa, showed some residual or even increased variability biases post-correction. Several potential reasons were considered as follows. The observed standard deviation in these regions is very low (e.g., due to low moisture variability or stable conditions), and the correction may overcompensate when adjusting GCM variability. Multivariate 440 corrections can induce indirect changes to a variable due to its coupling with others (e.g., correcting q in relation to ta). If temperature or wind speed is also adjusted in a way that enhances moisture variability, it could introduce an increased standard deviation in specific humidity, even if the raw bias was negative. It's also possible that the raw GCM's low variability was an artifact of its dynamics, while SDMBCv2 aligns the variability closer to ERA5. These aspects warrant



445 further exploration, especially in areas with low variability that may diminish the effectiveness of multivariate bias correction performance.

Another crucial strength of SDMBCv2 is its ability to maintain observed temporal and multivariate structures in GCM outputs. Lag-1 autocorrelation analysis indicated significant reductions in biases related to temporal persistence, highlighting the software's capability to prevent unrealistic short-term memory effects in the climate system. Additionally, SDMBCv2 maintained accurate cross-correlations among variables where uncorrected simulations showed substantial errors. For 450 instance, the original GCM overestimated the coupling between air temperature and specific humidity, potentially inflating convective feedback; SDMBCv2 effectively corrected these interdependencies.

The validation period results further confirmed the robustness and generalizability of SDMBCv2. Bias corrections derived from the calibration period remained effective when applied to an independent validation period, maintaining similar levels of accuracy and consistency across multiple metrics. The Kolmogorov–Smirnov (K–S) tests provided strong statistical 455 confirmation, showing marked improvements in distributional alignment between the corrected GCM outputs and ERA5. Specifically, the SDMBC-corrected datasets demonstrated consistently high rates of passing the K–S test across all variables and times, contrasting sharply with the relatively poor performance of the raw GCM data.

Despite the notable improvements provided by SDMBCv2, several challenges remain. First, the correction quality inherently depends on the accuracy and reliability of observational benchmarks (here, ERA5). Areas with limited in-situ observations 460 or regions reliant primarily on satellite-based or modeled reanalysis products may present inherent uncertainties that propagate into the correction. Secondly, while SDMBCv2 generally preserves multivariate physical relationships, complex interactions in dynamically active or convectively dominant regions can pose challenges, potentially leading to locally increased biases. These aspects highlight the necessity for cautious interpretation of corrected outputs and further methodological refinements to address specific regional issues.

465 Future work should aim at reducing residual uncertainties and further enhancing the robustness of multivariate corrections. Integrating multiple observational datasets, potentially including satellite retrievals, could help provide more robust reference climatologies, particularly in poorly observed regions. Additionally, exploring advanced correction methodologies that better handle skewed or intermittent variables may further refine the representation of variability and extremes (Mehrotra and Sharma (2019), (Mehrotra and Sharma, 2021)).

470 In conclusion, SDMBCv2 provides a powerful, flexible, and reliable tool for addressing systematic biases in GCM boundary conditions for regional climate modeling. SDMBCv2 facilitates improved climate modeling efforts, directly benefiting applications such as infrastructure planning, water resource management, and climate risk assessments. Continued development and refinement of this software promise further improvements in the fidelity and utility of regional climate simulations.

475



Code, data, or code and data availability

The example input and output datasets used in this study are archived on Zenodo and available at <https://doi.org/10.5281/zenodo.17577882>. Due to data volume constraints, the full datasets are not publicly archived but may be made available upon reasonable request from the corresponding authors. The bias-correction framework developed in this
480 study, SDMBCv2, is openly available at https://github.com/young-ccrc/sdmvc_v2, including all scripts required to reproduce the methodology. ERA5 reanalysis data were obtained from the Copernicus Climate Data Store and are available via Hersbach et al. (2023) at <https://doi.org/10.24381/cds.bd0915c6>, subject to the Licence to Use Copernicus Products. ACCESS-ESM1.5 global climate model data were obtained from the CMIP6 archive and are available via Ziehn et al. (2019) at <https://doi.org/10.22033/ESGF/CMIP6.4272>, distributed under the Creative Commons Attribution 4.0 International
485 License (CC BY 4.0).

Author contributions

Y.K. conceived the study, developed the SDMBCv2 methodology and the software, performed the simulations and analyses, curated the datasets, and wrote the original manuscript. J.P.E. supervised the research, contributed to the conceptual development and interpretation of the results, and reviewed and edited the manuscript.

490 Competing interests

The authors declare that they have no known competing financial interests or personal relationships that could have influenced the work reported in this paper.

Acknowledgements

The authors acknowledge Han Liao for testing the SDMBCv2 software, analyzing its performance, and providing valuable
495 feedback that contributed to improving the robustness and usability of the framework. The authors also acknowledge Ashish Sharma for his supervisory contributions to the earlier development of the SDMBC framework, which informed the foundations of this work. This research was undertaken with the assistance of resources from the National Computational Infrastructure (NCI Australia), an NCRIS-enabled capability supported by the Australian Government.

Financial support

500 Y.K. and J.P.E. were supported via the ARC Centre of Excellence for Climate Extremes (CE170100023) and the Australian Government under the National Environmental Science Program.



References

Bruyere, C. L., Done, J. M., Holland, G. J., and Fredrick, S.: Bias corrections of global models for regional climate simulations of high-impact weather, *Climate Dynamics*, 43, 1847-1856, 10.1007/s00382-013-2011-6, 2014.

505 Cannon, A. J.: Multivariate Bias Correction of Climate Model Output: Matching Marginal Distributions and Intervariable Dependence Structure, *Journal of Climate*, 29, 7045-7064, 10.1175/Jcli-D-15-0679.1, 2016.

Cannon, A. J.: Multivariate quantile mapping bias correction: an N-dimensional probability density function transform for climate model simulations of multiple variables, *Climate Dynamics*, 50, 31-49, 10.1007/s00382-017-3580-6, 2018.

510 Hersbach, H., Bell, B., Berrisford, P., Hirahara, S., Horanyi, A., Munoz-Sabater, J., Nicolas, J., Peubey, C., Radu, R., Schepers, D., Simmons, A., Soci, C., Abdalla, S., Abellán, X., Balsamo, G., Bechtold, P., Biavati, G., Bidlot, J., Bonavita, M., De Chiara, G., Dahlgren, P., Dee, D., Diamantakis, M., Dragani, R., Flemming, J., Forbes, R., Fuentes, M., Geer, A., Haimberger, L., Healy, S., Hogan, R. J., Holm, E., Janiskova, M., Keeley, S., Laloyaux, P., Lopez, P., Lupu, C., Radnoti, G., de Rosnay, P., Rozum, I., Vamborg, F., Villaume, S., and Thepaut, J. N.: The ERA5 global reanalysis, *Q J Roy Meteor Soc*, 146, 1999-2049, 10.1002/qj.3803, 2020.

515 Johnson, F. and Sharma, A.: A nesting model for bias correction of variability at multiple time scales in general circulation model precipitation simulations, *Water Resources Research*, 48, Artn W01504 10.1029/2011wr010464, 2012.

Kim, Y., Evans, J. P., and Sharma, A.: Multivariate bias correction of regional climate model boundary conditions, *Climate Dynamics*, 10.1007/s00382-023-06718-6, 2023a.

520 Kim, Y., Evans, J. P., and Sharma, A.: Correcting biases in regional climate model boundary variables for improved simulation of high-impact compound events, *Iscience*, 26, ARTN 107696 10.1016/j.isci.2023.107696, 2023b.

525 Kim, Y., Evans, J. P., and Sharma, A.: Can Sub-Daily Multivariate Bias Correction of Regional Climate Model Boundary Conditions Improve Simulation of the Diurnal Precipitation Cycle?, *Geophysical Research Letters*, 50, ARTN e2023GL104442 10.1029/2023GL104442, 2023c.

Kim, Y., Evans, J. P., and Sharma, A.: A software for correcting systematic biases in RCM input boundary conditions, *Environ Modell Softw*, 168, ARTN 105799 10.1016/j.envsoft.2023.105799, 2023d.

530 Kim, Y., Evans, J. P., Sharma, A., and Rocheta, E.: Spatial, Temporal, and Multivariate Bias in Regional Climate Model Simulations, *Geophysical Research Letters*, 48, 10.1029/2020gl092058, 2021.

Kim, Y. and Evans, J.: SDMBC v2 – Input and Output Datasets (Version 1.0). Zenodo [data set], doi:10.5281/zenodo.17577882, 2025.

Mehrotra, R. and Sharma, A.: An improved standardization procedure to remove systematic low frequency variability biases 535 in GCM simulations, *Water Resources Research*, 48, Artn W12601 10.1029/2012wr012446, 2012.

Mehrotra, R. and Sharma, A.: Correcting for systematic biases in multiple raw GCM variables across a range of timescales, *J Hydrol*, 520, 214-223, 10.1016/j.jhydrol.2014.11.037, 2015.

540 Mehrotra, R. and Sharma, A.: A Resampling Approach for Correcting Systematic Spatiotemporal Biases for Multiple Variables in a Changing Climate, *Water Resources Research*, 55, 754-770, 10.1029/2018wr023270, 2019.

Mehrotra, R. and Sharma, A.: A robust alternative for correcting systematic biases in multi-variable climate model simulations, *Environ Modell Softw*, 139, ARTN 105019 10.1016/j.envsoft.2021.105019, 2021.

545 Mehrotra, R., Johnson, F., and Sharma, A.: A software toolkit for correcting systematic biases in climate model simulations, *Environ Modell Softw*, 104, 130-152, 10.1016/j.envsoft.2018.02.010, 2018.

Rahimi, S., Huang, L., Norris, J., Hall, A., Goldenson, N., Risser, M., Feldman, D. R., Lebo, Z. J., Dennis, E., and Thackeray, C.: Understanding the Cascade: Removing GCM Biases Improves Dynamically Downscaled Climate Projections, *Geophysical Research Letters*, 51, 10.1029/2023gl106264, 2024.

Risser, M. D., Rahimi, S., Goldenson, N., Hall, A., Lebo, Z. J., and Feldman, D. R.: Is Bias Correction in Dynamical 550 Downscaling Defensible?, *Geophysical Research Letters*, 51, ARTN e2023GL105979



10.1029/2023GL105979, 2024.

Rocheta, E., Evans, J. P., and Sharma, A.: Can Bias Correction of Regional Climate Model Lateral Boundary Conditions Improve Low-Frequency Rainfall Variability?, *Journal of Climate*, 30, 9785-9806, 10.1175/jcli-d-16-0654.1, 2017.

Salas, J. D.: Applied modeling of hydrologic time series, *Water Resources Publication* 1980.

555 Sharma, A. and Lall, U.: A nonparametric approach for daily rainfall simulation, *Math Comput Simulat*, 48, 361-371, Doi 10.1016/S0378-4754(99)00016-6, 1999.

Srikanthan, R. and Pegram, G. G. S.: A nested multisite daily rainfall stochastic generation model, *J Hydrol*, 371, 142-153, 10.1016/j.jhydrol.2009.03.025, 2009.

560 Tabari, H., Paz, S. M., Buekenhout, D., and Willems, P.: Comparison of statistical downscaling methods for climate change impact analysis on precipitation-driven drought, *Hydrol Earth Syst Sc*, 25, 3493-3517, 10.5194/hess-25-3493-2021, 2021.

Xu, Z. and Yang, Z.-L.: An Improved Dynamical Downscaling Method with GCM Bias Corrections and Its Validation with 30 Years of Climate Simulations, *Journal of Climate*, 25, 6271-6286, 10.1175/jcli-d-12-00005.1, 2012.

Ziehn, T., Chamberlain, M. A., Law, R. M., Lenton, A., Bodman, R. W., Dix, M., Stevens, L., Wang, Y. P., and Srbinovsky, J.: The Australian Earth System Model: ACCESS-ESM1.5, *J So Hemisph Earth*, 70, 193-214, 10.1071/Es19035, 2020.

565